

Detecting Solenoidal Plasma Turbulence via Laser Polarization Rotation

Kenan Qu and Nathaniel J. Fisch

Department of Astrophysical Sciences, Princeton University, Princeton, New Jersey 08544, USA

(Dated: January 28, 2026)

Recent theoretical studies suggest that solenoidal turbulence can significantly enhance fusion reactivity, yet no standard diagnostic exists to directly measure these solenoidal flows in high-energy-density plasmas, nor to distinguish between solenoidal and compressional turbulence. We propose a method that directly diagnoses the energy and spatial structure of this rotational turbulence using the cross-polarization scattering of a probe laser. By coupling to the plasma vorticity, the scattering generates a cross-polarized signal proportional to the turbulent vorticity, effectively acting as a calorimeter for shear flows. We identify a diffractive scattering signature analogous to “Debye-Scherrer ring” that reveals the eddy size distribution. We show that this technique is applicable to National Ignition Facility (NIF) implosion conditions and other high-energy-density scenarios.

Introduction— Turbulence plays a central role in the dynamics of high-energy-density (HED) plasmas, particularly in the context of Inertial Confinement Fusion (ICF). Physically, turbulent flows decompose into two distinct components: compressional modes ($\nabla \cdot \mathbf{u} \neq 0$, where \mathbf{u} is the fluid velocity), associated with density fluctuations, and solenoidal or rotational modes ($\nabla \times \mathbf{u} \neq 0$), which manifest as shear flows and vortices [1, 2]. Historically, experimental diagnostics have focused heavily on the compressional component. Tools such as Thomson scattering, interferometry, and radiometry are highly sensitive to electron density fluctuations, making the measurement of compressional turbulence relatively straightforward [3, 4]. Various implementations of these techniques, such as Doppler backscattering and cross-polarization scattering (for magnetic fluctuations), have been successfully deployed in magnetic fusion devices to characterize density turbulence [5–12].

However, the recently proposed “shear flow reactivity enhancement effect” suggests that solenoidal turbulence can significantly boost fusion reactivity beyond levels expected from thermalization alone [13, 14]. In this regime, fast ions with long mean free paths sample differing bulk velocities across turbulent eddies, effectively increasing the center-of-mass collision energy. This finding challenges the conventional view that imploding plasmas must fully thermalize to maximize yield and suggests that embracing, rather than avoiding, shear flow turbulence could lower the ignition threshold.

In view of this possibly profound paradigmatic shift, a major experimental gap is exposed: there are no established, non-intrusive methods to directly detect and quantify these shear flows in dense HED plasmas [15, 16]. Because solenoidal motions are incompressible to first order in the turbulent energy, they do not generate the density fluctuations required for standard scattering techniques. Without a diagnostic capable of isolating the rotational component of turbulence, experimental verification of these shear-flow theories remains elusive.

Polarimetry offers a promising path forward. As a diagnostic technique sensitive to the polarization

of the electromagnetic field, it is inherently well-suited for detecting transverse fluctuations in the plasma medium, such as shear flows. However, the application of polarimetry to unmagnetized turbulence has been historically overlooked. In conventional plasma diagnostics, polarization rotation is almost exclusively associated with the presence of a background magnetic field (known as Faraday rotation [17–19]), leading to the widespread assumption that polarimetry is ineffective in unmagnetized HED environments.

This assumption stems from a reliance on magnetic gyrotropy. It is often assumed that unmagnetized plasmas, lacking this symmetry breaking, would not exhibit such polarization effects. However, recent work by Guérout and Langlois [20, 21] has demonstrated that a rotating unmagnetized plasma possesses an effective gyrotropy due to inertial forces, *i.e.*, the Coriolis effect. This polarization drag effect allows us to build a diagnostic tool specifically sensitive to plasma vorticity.

While previous work established the fundamental mechanism for coherent, rigid-body rotation of a bulk plasma, the implications for random, multiscale turbulence have remained unexplored. Here, we propose utilizing this mechanism as a targeted diagnostic for solenoidal turbulence. We demonstrate that plasma fluid *vorticity* acts as a source term for electromagnetic scattering, thereby modifying the polarization state of a probe beam. Unlike the coherent rotation described by Guérout *et al.*, we describe an effect where randomly distributed turbulent eddies cause an incoherent accumulation of polarization rotation, manifesting as a measurable rms spreading of the polarization angle. This allows the energy of the rotational velocity field to be inferred directly from the cross-polarized scattered light, independent of density fluctuations. Furthermore, we exploit the diffractive nature of this scattering, specifically the formation of Debye-Scherrer rings, to determine the spatial scale of the turbulence from the ring’s opening angle.

Thus, by simultaneously retrieving the two scalar quantities of solenoidal turbulence that govern the

shear flow reactivity enhancement effect—the energy magnitude and its characteristic scale—this methodology enables the key 3D tomographic reconstruction of the turbulence.

Mechanism of Polarization Rotation— The polarization rotation can be seen by considering the different phase velocities of circular polarization components in the rotating frame. A linearly polarized wave can be decomposed into right-hand and left-hand circular components. In a frame rotating at ω_{rot} , each component experiences a rotational Doppler frequency shift $\Delta\omega = \pm\omega_{\text{rot}}$, leading to a phase velocity difference $\pm(\omega_p^2/\omega_L^2)(\omega_{\text{rot}}t/2)$, where ω_p is the plasma frequency and ω_L is the laser frequency. This differential phase accumulation results in a polarization rotation angle

$$\psi = \frac{L}{cn} \frac{n_e}{n_c} \omega_{\text{rot}}, \quad (1)$$

where L is the interaction length, c is the speed of light, n_e is the electron density, $n_c = m_e \epsilon_0 \omega_L^2 / e^2$ is the critical plasma density, $\eta = \sqrt{1 - n_e/n_c}$ is the non-relativistic refractive index, m_e is the electron rest mass, ϵ_0 is the vacuum permittivity, and e is the natural charge. The scattering depends on three factors: the fluid vorticity Ω , the plasma density n_e , and the refractive index η . Critically, the scattering is amplified for plasma near the critical density ($\eta \rightarrow 0$). The reduced laser group velocity increases the interaction time as the beam traverses the plasma turbulence.

The effect of a rotating rigid medium dragging the plane of polarization of light passing through it was investigated under the term “Fresnel drag” by Fermi [22], and later by Jones [23] and Player [24]. The theory was recently extended to plasmas by Guérout *et al.* [20] by assuming that the dielectric conductivity tensor transforms rigidly with plasma rotation. It can be demonstrated that this polarization rotation angle is robust at temperatures in a fusion environment.

Depolarization due to Incoherent Scattering— Equation (1) applies if the entire plasma rotates as a rigid body. However, in realistic plasma turbulence, the vorticity field $\omega_{\text{rot}}(\mathbf{x})$ is not a single coherent structure but a collection of random eddies. This process is most accurately described as a random rotation of the polarization angle. As the laser propagates through the plasma, it encounters a sequence of uncorrelated vortices, each imparting a small, random polarization rotation $\delta\psi$. Physically, this manifests as depolarization: a linearly polarized beam broadens into an elliptical distribution with a variance proportional to the interaction length, as illustrated in Fig. 1.

If the size of each eddy is l_{eddy} , the accumulated polarization change after interacting with $N = L/l_{\text{eddy}}$

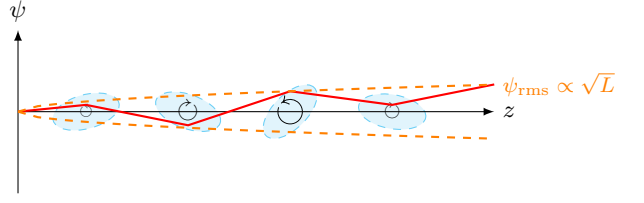


FIG. 1. Random walk of the polarization angle ψ as the laser beam traverses multiple uncorrelated turbulent eddies, leading to an rms broadening ψ_{rms} .

eddies follows a random walk

$$\langle \Delta\psi^2 \rangle = \sum_{i=1}^N \langle \delta\psi_i^2 \rangle = \left(\frac{1}{cn} \frac{n_e}{n_c} \omega_{\text{rot}} \right)^2 L l_{\text{eddy}}. \quad (2)$$

Consequently, the rms rotation angle $\psi_{\text{rms}} = \sqrt{\langle \Delta\psi^2 \rangle}$ scales with the square root of the interaction length.

Diagnostic of Turbulent Energy— We can invert these relations to serve as a diagnostic for the kinetic energy of the plasma turbulence. The turbulent kinetic energy density W_{turb} is defined as $W_{\text{turb}} = \frac{1}{2} m_e n_e \langle u^2 \rangle$. Assuming isotropic turbulence, the vorticity magnitude is defined by the velocity shear at the eddy scale, $\omega_{\text{rot}} \approx u_{\text{rms}}/l_{\text{eddy}}$ (assuming eddies have comparable transverse and longitudinal dimensions). We then find a scaling relation dependent on the turbulence parameters

$$\psi_{\text{rms}} = \frac{\sqrt{2}}{cn} \left(\frac{n_e}{n_c} \right) \sqrt{\frac{L}{l_{\text{eddy}}}} \sqrt{\frac{W_{\text{turb}}}{m_e n_e}}. \quad (3)$$

The polarization rotation ψ gives rise to a cross-polarized electric field $E_{\perp} = E_{\text{in}} \sin \psi \approx E_{\text{in}} \psi$, implying that the measured power fraction scales quadratically with the angle, $P_{\perp}/P_{\text{in}} \approx \psi_{\text{rms}}^2$. In an experiment, one typically measures the total power or energy of the cross-polarized light (P_{\perp}) relative to the incident power (P_{in})

$$\frac{P_{\perp}}{P_{\text{in}}} = \frac{2W_{\text{turb}}}{m_e c^2 \eta^2} \left(\frac{n_e}{n_c^2} \right) \left(\frac{L}{l_{\text{eddy}}} \right). \quad (4)$$

The scattered power ratio is linearly proportional to the total turbulent kinetic energy. Thus, the cross-polarized detector acts as a calorimeter for plasma turbulence. To obtain the turbulence energy density W_{turb} , one requires the plasma density n_e (measurable via standard Thomson scattering or interferometry) and the eddy size l_{eddy} . In the following section, we describe how l_{eddy} can be measured directly from the scattering geometry.

Relation between Scattering Angle and Eddy Size— The frequency-conserving scattering process due to random plasma turbulence can be treated as the elastic diffraction of a coherent input. While the total cross-polarized power is a calorimetric measure of the energy, the spatial structure of the scattering encodes the geometric properties of the turbulence.

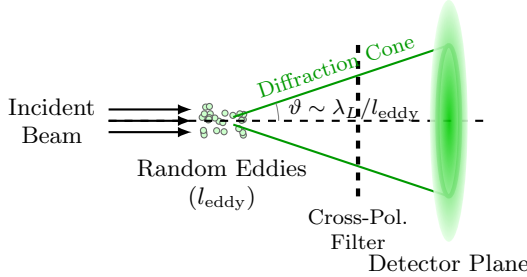


FIG. 2. Randomly oriented eddies of a characteristic size l_{eddy} produce a diffraction cone. A distribution of rings is formed behind a cross-polarization filter, analogous to a Debye-Scherrer ring.

The collective scattering of eddies with characteristic size l_{eddy} produces a cone-shaped diffraction pattern. Eddies with a distribution of sizes will form a distribution of rings (or a diffuse halo), where each radial angle ϑ corresponds to a specific eddy size l_{eddy} in the spectrum. The scattered field is proportional to the Fourier transform of the vorticity field $\Omega(\mathbf{q})$ evaluated at the scattering vector $\mathbf{q} = \mathbf{k}_s - \mathbf{k}_L$, defined by the scattered (\mathbf{k}_s) and incident (\mathbf{k}_L) wave vectors. For isotropic turbulence characterized by a dominant eddy scale l_{eddy} , the vorticity power spectrum $S_\Omega(\mathbf{q}) = \langle |\Omega(\mathbf{q})|^2 \rangle$ is concentrated in a spherical shell in k -space with radius $q_0 = 2\pi/l_{\text{eddy}}$. Elastic scattering conserves frequency, *i.e.*, $|\mathbf{k}_s| = |\mathbf{k}_L| = k_L$. Geometrically, this constrains the scattering vector \mathbf{q} to lie on the intersection of the Ewald sphere (radius k_L) and the turbulence spectral shell. This intersection defines a cone of angle ϑ relative to the \mathbf{k}_L direction

$$q = 2k_L \sin(\vartheta/2) = q_0. \quad (5)$$

For small scattering angles, this simplifies to the Bragg-like condition

$$\vartheta \approx \frac{q_0}{k_L} = \frac{\lambda_L}{l_{\text{eddy}}}, \quad (6)$$

where λ_L is the laser wavelength. For isotropic turbulence with random eddy orientations, the scattering is azimuthally symmetric around the laser axis. To isolate this signal, a cross-polarization filter is placed in the beam path, extinguishing the coherent unscattered light while transmitting the rotationally scattered components.

If the turbulence possesses a single dominant length scale, the scattered light forms a distinct ring on a downstream detector, analogous to the Debye-Scherrer rings observed in X-ray powder diffraction [25]. For vortices with totally random sizes, the rings would diffuse into a filled disk. However, even in this diffuse case, the signal at a specific radius (angle ϑ) still corresponds to a specific eddy size $l_{\text{eddy}} \approx \lambda_L/\vartheta$, and the angular

intensity profile $I(\vartheta)$ allows for the reconstruction of the turbulence size distribution $S(l_{\text{eddy}}) \propto \vartheta^2 I(\vartheta)$. Thus, by measuring the radial profile of the Debye-Scherrer pattern in the cross-polarized channel, one can directly measure the power spectrum of the turbulent eddies.

It is crucial to decouple the information contained in the ring's geometry from its brightness. The ring radius (angle ϑ) is determined by the eddy size l_{eddy} via diffraction; smaller eddies scatter light to wider angles. Measuring the ring radius provides the spatial scale of the turbulence l_{eddy} , which can then be substituted back into Eq. (5) to isolate the turbulent energy density. The ring brightness, on the other hand, is determined by the vorticity magnitude and plasma density. A more energetic vortex makes the ring brighter but does not change its diameter.

The spectral width of the diffraction ring provides a measurement of the turbulence kinematics that is complementary to the polarization rotation method. While the polarization rotation (manifesting as the total cross-polarized power) yields a calorimetric measure of the turbulent energy ($P_\perp \propto n_e^2 u_{\text{rms}}^2$), the spectral linewidth independently encodes the velocity distribution. Since the scattering vector magnitude q_0 is fixed by the ring angle, the spectral lineshape is determined by the Doppler broadening from the random eddy velocities, scaling as $\Delta\omega_{\text{ring}} \approx q_0 u_{\text{rms}}$. Thus, spectrally resolving the ring allows one to extract the vorticity magnitude $|\Omega|$ and verify the fluid velocity scale separate from the signal brightness.

This spectral signature is also useful for isolating the turbulence from the thermal background. Although the collected light is an incoherent sum of scattering from many eddies, resulting in a broadened peak, this peak remains distinct because of the separation of velocity scales. In typical HED conditions, the electron thermal velocity (v_{th}) exceeds the fluid velocity (u_{rms}) by orders of magnitude ($v_{\text{th}} \gg u_{\text{rms}}$). Consequently, the thermal electrons produce a wide, diffuse spectral pedestal ($\Delta\omega_{\text{th}} \sim kv_{\text{th}}$), whereas the vorticity scattering appears as a comparatively narrow peak ($\Delta\omega_{\text{ring}} \sim ku_{\text{rms}}$) superimposed on top. However, if the fluid velocity were to approach the thermal velocity ($u_{\text{rms}} \rightarrow v_{\text{th}}$), the spectral broadening of the turbulence would become comparable to the thermal width. In this limit, the distinctive narrow peak would widen and vanish into the thermal noise floor, making the diagnostic ineffective.

Numerical Examples and Experimental Feasibility— To assess the practicality of this diagnostic, we evaluate the expected signal strength for three distinct experimental regimes in HED physics. The primary metrics are the rms polarization rotation angle ψ_{rms} , the cross-polarized intensity ratio P_\perp/P_{in} , and the Debye-Scherrer ring angle ϑ . The results are summarized in Table I.

Case A: NIF Implosion. This scenario represents the

TABLE I. Summary of Feasibility Estimates

Parameter	Case A (NIF)	Case B (Ablation)	Case C (Far-IR) (Gas Jet)
Probe λ	30 nm	0.33 μm	33 μm
Density n_e	10^{24} cm^{-3}	10^{22} cm^{-3}	10^{18} cm^{-3}
Refr. Index η	0.1	0.14	0.1
Eddy Size l_{eddy}	1 μm	7 μm	2 mm
Interactions N	50	57	1
Flow Vel. u	300 km/s	6 km/s	2 km/s
Pol. Rot. $\delta\psi$	10 mrad	0.15 mrad	0.07 mrad
RMS Rotation	70 mrad	1.1 mrad	0.07 mrad
Intensity Ratio	5×10^{-3}	10^{-6}	5×10^{-9}
Ring Angle ϑ	30 mrad	47 mrad	17 mrad

most promising application. In ICF experiments at the National Ignition Facility (NIF), the mix layer between the shell and fuel is extremely dense ($n_e \sim 10^{24} \text{ cm}^{-3}$) and turbulent [16]. We assume a soft X-ray probe ($\lambda \approx 30 \text{ nm}$) chosen to be close to the plasma frequency of the mix layer ($n_e/n_c \approx 0.99$). The interaction in this regime is dominated by the proximity to the critical density. As $n_e \rightarrow n_c$, the refractive index η drops to ~ 0.1 . The slow group velocity dramatically increases the interaction time and effective coupling efficiency between the probe and the turbulence, amplifying the scattered signal significantly compared to underdense interactions.

A critical requirement for this diagnostic is a probe beam with a high degree of initial linear polarization. For the X-ray regime, several sources can provide the necessary polarization purity. Synchrotron radiation and X-ray Free Electron Lasers (XFEL) are naturally highly polarized with extinction ratios below 10^{-5} [26, 27]. Laser-produced High Harmonic Generation (HHG) sources are also ideal as they inherit the linear polarization of the drive laser with high fidelity, achieving extinction ratios better than 10^{-4} . Alternatively, one can use crystal optics based on Bragg reflection at 45° to purify the polarization of thermal X-ray sources [28].

Regarding detection, the incoherent accumulation over $N \approx 50$ interactions yields a rotation $\psi_{\text{rms}} \sim 70$ mrad. This corresponds to a cross-polarized intensity ratio $P_{\perp}/P_{\text{in}} \approx 5 \times 10^{-3}$. Assuming an input X-ray pulse with 10^{12} photons, the cross-polarized signal would contain $\sim 5 \times 10^9$ photons, a signal easily distinguishable from noise. Even if the signal is weakened by plasma lensing effects, it would remain above the extinction floor of input polarization. The expected ring angle is $\vartheta \approx 30 \text{ nm}/1 \mu\text{m} \approx 0.03 \text{ rad (1.7}^\circ)$. This angle allows the scattered signal to be spatially separated from the main beam while remaining within the collection cone of standard area detectors.

Case B: Turbulent Laser-Produced Plasma. This case corresponds to recent experiments studying turbulence in laser-produced plasmas [29], where a shock driven into

a low-density foam target generates a turbulent mixing zone. The characteristic plasma parameters observed are an electron density $n_e \approx 10^{22} \text{ cm}^{-3}$ and a fluid velocity $u \approx 6 \text{ km/s}$. The characteristic turbulence scale length, identified as the spectral knee, is $l_{\text{eddy}} \approx 7 \mu\text{m}$, and the plasma extension is $L \approx 400 \mu\text{m}$. To probe this high-density plasma, we propose using a UV probe ($\lambda = 0.33 \mu\text{m}$, e.g., a frequency-tripled Nd:YAG laser or excimer laser). The estimated rms rotation is $\psi_{\text{rms}} \approx 1.1 \text{ mrad}$, corresponding to an intensity ratio of $P_{\perp}/P_{\text{in}} \sim 1.2 \times 10^{-6}$. While weaker than the resonant NIF case due to the lower flow velocity, this signal is well within the range of standard high-extinction polarimetry, making detection feasible. The diffractive ring angle $\vartheta \approx 0.33 \mu\text{m}/7 \mu\text{m} \approx 47 \text{ mrad (2.7}^\circ)$ is well-suited for detection.

Case C: Gas Jet. This scenario is typical of laser wakefield acceleration experiments using low-density gas targets. Using a standard infrared probe ($\lambda = 0.8 \mu\text{m}$), the predicted signal is $\psi \approx 50 \mu\text{rad}$, corresponding to an intensity ratio of $P_{\perp}/P_{\text{in}} \sim 10^{-9}$. This level is practically unmeasurable due to photon statistics and background noise. However, by utilizing a far-IR probe (e.g., $\lambda = 33 \mu\text{m}$), we can tune the diagnostic to the critical density of the tenuous plasma ($n_c \approx 10^{18} \text{ cm}^{-3}$). With this resonant enhancement ($\eta \approx 0.1$), the signal is dramatically boosted. The rms rotation angle increases to $\psi_{\text{rms}} \approx 0.07 \text{ mrad}$, corresponding to an intensity ratio of $P_{\perp}/P_{\text{in}} \approx 5 \times 10^{-9}$. This renders the measurement feasible, demonstrating the versatility of the method across density regimes. The ring angle would be $\vartheta \approx 33 \mu\text{m}/2 \text{ mm} \approx 17 \text{ mrad (1}^\circ)$.

Discussion and Conclusion— We showed how laser polarization rotation can diagnose plasma turbulence, specifically targeting the vortical component critical to fusion yield. The method is particularly useful because it scales with the energy of the turbulence rather than merely the density fluctuations. By measuring the total power of the cross-polarized scattered light, one obtains a calorimetric measurement of the turbulent kinetic energy. In HED regimes, specifically near-critical plasmas like those in NIF implosions, the effect is resonantly enhanced, offering a unique window into the dynamics of hydrodynamic instabilities that are otherwise invisible to standard diagnostics. Critically, this diagnostic bridges the gap between turbulence theory and fusion performance.

The extracted values of turbulent kinetic energy W_{turb} and eddy size l_{eddy} are the precise inputs required to evaluate the “shear flow reactivity enhancement” factor predicted by Fetsch and Fisch [13]. By quantifying W_{turb} , one can estimate the effective temperature increase experienced by reacting ions, thereby directly determining whether the turbulence is acting as a deleterious energy sink or a beneficial reactivity booster. This capability could be pivotal for optimizing ignition

designs that leverage, rather than suppress, shear flows.

However, several experimental challenges must be addressed. A primary concern in HED plasmas is refraction due to large density gradients. As the probe beam approaches the critical density to maximize the signal, small density fluctuations can cause significant beam steering and distortion. This lensing effect modifies the effective scattering angle ϑ and can potentially mask the diffractive ring signature. Advanced ray-tracing simulations would be necessary to deconvolve these refractive effects from the turbulence scattering signal. Additionally, operating near the critical density enhances collisional absorption (inverse Bremsstrahlung), which may attenuate the probe beam and reduce the signal-to-noise ratio.

Another potential complication is the presence of spontaneous magnetic fields, which are common in laser-produced plasmas through, e.g., the Biermann battery effect [30]. These fields induce Faraday rotation, which also rotates the polarization plane. However, Faraday rotation is a coherent, path-integrated effect that typically scales with λ^2 or operates differently in the X-ray regime, whereas the vorticity scattering discussed here is an incoherent, diffusive process with diffraction rings. Distinguishing the two may require multi-wavelength probing or spatial filtering to isolate the scattered halo from the coherent main beam rotation.

Despite these caveats, it remains that this methodology offers a tool uniquely suited to diagnose directly solenoidal turbulence. Furthermore, by employing multiple probe beams at different angles and polarization states, it is theoretically possible to reconstruct the three-dimensional vorticity vector field $\Omega(\mathbf{x})$ using vector tomography techniques [31–33], analogous to methods used in medical imaging and tokamak SXR diagnostics.

This work was supported by NNSA Grant No. DE-NA0004167.

the DIII-D tokamaka), *Review of Scientific Instruments* **81**, 10D912 (2010).

- [6] T. L. Rhodes, W. A. Peebles, N. A. Crocker, and X. Nguyen, Development of a cross-polarization scattering system for the measurement of internal magnetic fluctuations in the DIII-D tokamaka), *Review of Scientific Instruments* **85**, 11D838 (2014).
- [7] K. Barada, T. L. Rhodes, N. A. Crocker, and W. A. Peebles, Measurement of local, internal magnetic fluctuations via cross-polarization scattering in the DIII-D tokamak (invited), *Review of Scientific Instruments* **87**, 11E601 (2016).
- [8] Z. B. Shi, W. L. Zhong, M. Jiang, G. L. Che, Z. C. Yang, P. W. Sun, B. Y. Chen, X. L. Li, W. Chen, and X. T. Ding, A novel multi-channel quadrature Doppler backward scattering reflectometer on the HL-2A tokamak, *Review of Scientific Instruments* **93**, 013501 (2022).
- [9] L. Zhang, J. Yu, J. Yang, G. Zhuang, and J. Xie, The commissioning progress of microwave imaging reflectometer on east tokamak, *Journal of Instrumentation* **20** (03), T03008.
- [10] X. L. Zou, L. Colas, M. Paume, J. M. Chareau, L. Laurent, P. Devynck, and D. Gresillon, Internal magnetic turbulence measurement in plasma by cross polarization scattering, *Phys. Rev. Lett.*.
- [11] T. Lehner, J. M. Rax, and X. L. Zou, Linear mode conversion by magnetic fluctuations in inhomogeneous magnetized plasmas, *Europhysics Letters* **8**, 759 (1989).
- [12] Y. Maron, Experimental determination of the thermal, turbulent, and rotational ion motion and magnetic field profiles in imploding plasmas, *Physics of Plasmas* **27**, 060901 (2020).
- [13] H. Fetsch and N. J. Fisch, Enhancement to fusion reactivity in sheared flows, *Physical Review Letters* **135**, 155101 (2025).
- [14] H. Fetsch and N. J. Fisch, Analytical models for the enhancement of fusion reactivity by turbulence, *Physics of Plasmas* **32**, 112703 (2025).
- [15] P. M. Nilson, J. Katz, M. Michalko, R. Raimondi, D. Guy, S. Klein, J. Schell, S. Zuhric, J. Robinson, C. Spindloe, J. Kendrick, D. T. Bishel, D. A. Chin, R. Beikirch, S. T. Ivancic, T. Cracium, A. Shvydky, S. Miller, T. J. B. Collins, R. Epstein, S. X. Hu, I. West-Abdalah, A. B. Sefkow, and D. H. Froula, Flow visualization in high-energy-density laboratory plasmas, *Physics of Plasmas* **32**, 082705 (2025).
- [16] B. A. Hammel, H. A. Scott, S. P. Regan, C. Cerjan, D. S. Clark, M. J. Edwards, R. Epstein, S. H. Glenzer, S. W. Haan, N. Izumi, J. A. Koch, G. A. Kyrala, O. L. Landen, M. M. Marinak, A. J. MacKinnon, N. B. Meezan, D. D. Meyerhofer, P. B. Radha, V. A. Smalyuk, L. J. Suter, and R. P. J. Town, High-mode Rayleigh-Taylor growth in NIF ignition capsules, *High Energy Density Physics* **6**, 171 (2010).
- [17] I. H. Hutchinson, *Principles of Plasma Diagnostics* (Cambridge University Press, 2002).
- [18] D. A. J. H., T. Edlington, E. Joffrin, H. R. Koslowski, C. Nieswand, S. E. Sege, P. E. Stott, and C. Walker, Poloidal polarimeter system for current density measurements in ITER, *Review of Scientific Instruments* **70**, 726 (1999).
- [19] S. E. Sege, A review of plasma polarimetry - theory and methods, *Plasma Physics and Controlled Fusion* **41**, R57

(1999).

[20] J. Langlois and R. Guérout, Signature of inertia on light dragging in rotating plasmas, arXiv preprint arXiv:2402.12050 (2024).

[21] J. Langlois and R. Guérout, Contribution of fictitious forces to polarization drag in rotating media, *Phys. Rev. E* **108**, 045201 (2023).

[22] E. Fermi, Sul trascinamento del piano di polarizzazione da parte di un mezzo rotante, *Rend. Mat. Acc. Lincei* **32**, 115 (1923).

[23] R. V. Jones, Rotary aether drag, *Proc. R. Soc. A* **349**, 423 (1976).

[24] M. A. Player, On the dragging of the plane of polarization of light propagating in a rotating medium, *Proc. R. Soc. A* **349**, 441 (1976).

[25] B. E. Warren, *X-ray diffraction* (Dover, 1990).

[26] K. S. Schulze, B. Grabiger, R. Loetsch, B. Marx-Glowina, A. T. Schmitt, A. L. Garcia, W. Hippler, L. Huang, F. Karbstein, Z. Konópková, H.-P. Schlenvoigt, J.-P. Schwinkendorf, C. Strohm, T. Toncian, I. Uschmann, H.-C. Wille, U. Zastrau, R. Röhlsberger, T. Stöhlker, T. E. Cowan, and G. G. Paulus, Towards perfectly linearly polarized x-rays, *Phys. Rev. Res.* **4**, 013220 (2022).

[27] A. A. Lutman, J. P. MacArthur, M. Ilchen, A. O. Lindahl, J. Buck, R. N. Coffee, G. L. Dakovski, L. Dammann, Y. Ding, H. A. Durr, L. Glaser, J. Grunert, G. Hartmann, N. Hartmann, D. Higley, K. Hirsch, Y. I. Levashov, A. Marinelli, T. Maxwell, A. Mitra, S. Moeller, T. Osipov, F. Peters, M. Planas, I. Shevchuk, W. F. Schlotter, F. Scholz, J. Seltmann, J. Viefhaus, P. Walter, Z. R. Wolf, Z. Huang, and H.-D. Nuhn, Polarization control in an x-ray free-electron laser, *Nature Photonics* **10**, 10.1038/nphoton.2016.79 (2016).

[28] B. Marx, K. S. Schulze, I. Uschmann, T. Kämpfer, R. Lötzsche, O. Wehrhan, W. Wagner, C. Detlefs, T. Roth, J. Härtwig, E. Förster, T. Stöhlker, and G. G. Paulus, High-Precision X-Ray Polarimetry, *Phys. Rev. Lett.* **110**, 254801 (2013).

[29] G. Rigon, B. Albertazzi, T. Michel, P. Mabey, V. Bouffetier, N. Ozaki, T. Pikuz, Y. Sakawa, A. Faenov, M. Koenig, and A. Casner, Micrometer-scale turbulence in laser-produced plasmas, *Nature Communications* **12**, 2679 (2021).

[30] J. A. Stamper, K. Papadopoulos, R. N. Sudan, S. O. Dean, E. A. McLean, and J. M. Dawson, Spontaneous magnetic fields in laser-produced plasmas, *Phys. Rev. Lett.* **26**, 1012 (1971).

[31] A. M. Cormack, Representation of a function by its line integrals, with some radiological applications. ii, *Journal of Applied Physics* **35**, 2908 (1964).

[32] R. S. Granetz and P. Smeulders, X-ray tomography on JET, *Nuclear Fusion* **28**, 457 (1988).

[33] J. L. Prince, Convolution backprojection formulas for 3d vector tomography, *IEEE Transactions on Image Processing* **5**, 71 (1996).